Entropy generation for forced convection in a porous saturated circular tube with uniform wall temperature

K. Hooman[1], A. Ejlali[2]

[1]School of Engineering, The University of Queensland, Brisbane, Australia (Correspondent Author)

[2]Fix Equipment Lead Engineer, Namavaran Delvar Engineering and Construction Company, Tehran, Iran

Abstract

A numerical study is reported to investigate both the First and the Second Law of Thermodynamics for thermally developing forced convection in a circular tube filled by a saturated porous medium, with uniform wall temperature, and with the effects of viscous dissipation included. A theoretical analysis is also presented to study the problem for the asymptotic region applying the perturbation solution of the Brinkman momentum equation reported by [1]. Expressions are reported for the temperature profile, the Nusselt number, the Bejan number, and the dimensionless entropy generation rate in the asymptotic region. Numerical results are found to be in good agreement with theoretical counterparts.

Keywords: Theoretical, Porous media, Bejan number, Brinkman number, Thermal development

Nomenclature

Be	Bejan number
Be*	average Bejan number
Br	Brinkman number
Br*	Darcy-Brinkman number
c_P	specific heat at constant pressure
Da	Darcy number, K/R^2
FFI	fluid friction irreversibility
G	negative of the applied pressure gradient
HTI	heat transfer irreversibility
k	effective thermal conductivity
K	permeability
M	μ_{eff}/μ
N	dimensionless temperature difference ($N=(T_{IN}-T_w)/T_w$)
Ns	dimensionless entropy generation
Ns*	average value of Ns
Nu	Nusselt number
Pe	Péclet number, $Pe=\rho c_p RU/k$
q"	wall heat flux
R	Tube radius
s	$(MDa)^{-1/2}$

$\dot{S}_{gen}$ entropy generation rate per unit volume

T* temperature

T_m bulk mean temperature, $T_m = 2\int_0^1 \hat{u}T^*rdr$

T_w wall temperature

u $\mu u^*/(GR^2)$

u* filtration velocity

$\hat{u}$ u*/U

U mean velocity, $U = 2\int_0^1 u^*rdr$

x* longitudinal coordinate

x x*/PeR

r* radial coordinate

r r*/R

Greek symbols

θ $(T^*-T_w)/(T_{IN}-T_w)$

μ fluid viscosity

μ_{eff} effective viscosity in the Brinkman term

ρ fluid density

1. Introduction

Analysis of fluid flow and heat transfer in porous ducts has been a subject of fundamental importance for being relevant to a lot of industrial applications [2]. There has been a renewed interest in the problem of forced convection through a porous passage for application of hyperporous medium in cooling electronic equipment. Meanwhile a great deal of information is available dealing with, and trying to minimize, the generated entropy due to heat and fluid flow in a porous passage [3-10]. Entropy generation minimization (EGM) is now a popular field of investigation since it aims at minimizing the lost work through decreasing the irreversibility of a system and, hence leads to an optimal design feature. Aiming at this goal, one should find the sources of entropy generation and correlate them with the known and measurable characteristics of the so-called system. One way of tackling the problem is to tie the results of the mass, momentum, and thermal energy balance to the Second Law (of Thermodynamics). Most of the newly-published articles follow the methodology of Bejan [11-13] to link the First Law and the Second Law, which assumes two possible sources of entropy generation being Heat Transfer Irreversibility (HTI) and Fluid Friction Irreversibility (FFI). The former is present in almost all of heat transfer devices due to heat transfer in finite temperature differences and the latter is responsible for dissipation of mechanical power to heat (viscous dissipation divided by the local absolute temperature). Modeling viscous dissipation in a porous medium is a controversial issue and there are three alternative models [14-17]. Recently, several authors have investigated the problem for forced convection through a circular tube saturated by a porous medium [18-22]. Hooman and co-workers [18-20] have only considered the Darcy dissipation term and neglected the velocity derivative terms. One knows that this assumption works out when the Darcy number is small [21-22].

Analytical solution for a thermally developing problem by numerical evaluation of the eigenvalues and eigenfunctions are reported in [21] while Haji-Sheikh et al. [22] have applied a Green's function solution to solve the same problem with an unheated entry length when the viscous dissipation is modeled similar to what proposed in [14].

None of the above articles dealt with the entropy generation analysis of the problem and nowhere else one can find a work addressing the issue, to the best knowledge of the authors. Moreover, in this paper explicit (without the need to numerical calculations) closed form solutions will be presented for both temperature profile and the Nusselt number which has not been reported in any of the above articles.

Previous work on the effects of viscous dissipation in ducts has been surveyed by Shah and London [23] and Magyari et al. [24] for the clear fluid and porous passages, respectively.

2. Analysis

For the steady-state fully developed situation we have unidirectional flow in the x*-direction inside a tube with impermeable wall at r* = R where the wall temperature, T_w, is constant, as illustrated in Fig 1-a.

The Brinkman momentum equation reads

$$\mu_{eff}\left(\frac{d^2u^*}{dr^{*2}}+\frac{1}{r^*}\frac{du^*}{dr^*}\right)-\frac{\mu}{K}u^*+G=0\,, \tag{1}$$

where μ_{eff} is an effective viscosity (here equal to the fluid viscosity μ), K is the permeability, and G is the negative of the applied pressure gradient. Similar to [1] the dimensionless velocity is defined as $u=\mu u^*/(GR^2)$ so that the dimensionless form of Eq. (1) is

$$M\left(\frac{d^2u}{dr^2}+\frac{1}{r}\frac{du}{dr}\right)-\frac{u}{\mathrm{Da}}+1=0. \tag{2}$$

Making use of the viscosity ratio M $(M=\mu_{eff}/\mu)$ and the Darcy number $(Da=K/R^2)$, the porous media shape factor is defined as $s=(MDa)^{-1/2}$ to rearrange Eq. (2) as

$$\frac{d^2u}{dr^2}+\frac{1}{r}\frac{du}{dr}-s^2u+\frac{1}{M}=0\,. \tag{3}$$

This equation has been solved subject to no slip boundary condition, i.e. u=0 at r=0, and the symmetry condition, i.e. du/dr=0 at r=0 and the asymptotic results are [1]

$$\hat{u}=2(1-r^2)[1+s^2(3r^2-1)/48], \quad \text{(for large Darcy number case)} \tag{4-a}$$

$$\hat{u}=(1+2/s)(1-r^{-1/2}e^{-s(1-r)}). \quad \text{(for small Darcy number case)} \tag{4-b}$$

Local thermal equilibrium and homogeneity is assumed. The steady state thermal energy equation in the absence of axial conduction and thermal dispersion (see [2] for the criteria based on which the above assumptions can come true) is

$$\rho c_p u^* \frac{\partial T^*}{\partial x^*} = \frac{k}{r^*}\frac{\partial}{\partial r^*}(r^* \frac{\partial T^*}{\partial r^*}) + \mu(\frac{u^{*2}}{K} + (\frac{du^*}{dr^*})^2) . \quad (5)$$

Introducing the Brinkman number $Br=\mu U^2/(k(T_{IN}-Tw))$, the dimensionless thermal energy equation is

$$\hat{u}\frac{\partial\theta}{\partial x} = \frac{\partial^2\theta}{\partial r^2} + \frac{1}{r}\frac{\partial\theta}{\partial r} + \mathrm{Br}(s^2\hat{u}^2 + (\frac{d\hat{u}}{dr})^2) . \quad (6)$$

The appropriate boundary conditions to solve the above equation are

$$\frac{\partial\theta}{\partial r}(x,0) = 0 \text{ and } \theta(x,1) = 0, \text{ (Crosswise)}$$
$$\theta(0,\mathrm{r}) = 1. \qquad \text{(Streamwise : Inlet)} \quad (7\text{-a,b})$$

Finally, the Nusselt number is defined as

$$\mathrm{Nu} = \frac{2Rq''}{k(T_w - T_m)} . \quad (8)$$

3. Thermal Entrance Region

An implicit finite difference scheme is applied to solve the thermal energy equation in the developing region, i.e. to solve Eq. (6) subject to the boundary conditions (7-a,b). The SY subroutine of [25] is applied to solve the tridiagonal system of algebraic equations resulting from our backward/central discretization in streamwise/transverse direction. The computational domain is a 1x1 box one which simulates the upper half of the tube shown in Fig. 1-a (due to symmetry above the tube centerline, i.e. r=0 line). One knows that this length is enough for the flow to become thermally fully developed [26]. One also notes that for this case the hydrodynamic entrance length is $O(K/\varepsilon)^{1/2}$, where ε is the porosity of the porous media. In most practical cases this is a small number and the problem is hydrodynamically fully developed through most of the flow region considered, for more details one can consult [27]. It was observed that a 91x91 mesh will lead to accurate results [19-22]. For *s*=316.227 ($Da=10^{-3}$) and *s*=1, Kuznetsov et al. [21] reported *Nu*=7.88 and *Nu*=8.206 while our fully developed *Nu* is 7.885 and 8.208, respectively. Besides, while with *s*=1 and *s*=10 Haji-Sheikh et al. [22] found *Nu* =8.209 and 6.172, our *Nu* is 8.208 and 6.169, respectively. With s=0 we found *Nu*=9.601 which is close to *Nu*=9.6 reported in [23]. Moreover, it was verified that the results are mesh independent since moving from a 91x91 mesh to a 121x121 one, Nu did not change within three significant figures.

4. Perturbation solutions

For large values of *x*, where the temperature shows no change with *x*, i.e. in the asymptotic region, the problem reduces to the following ordinary differential equation (subject to the boundary conditions (7-a))

$$\frac{\partial^2\theta}{\partial r^2} + \frac{1}{r}\frac{\partial\theta}{\partial r} + \mathrm{Br}(s^2\hat{u}^2 + (\frac{d\hat{u}}{dr})^2) = 0, \quad (9)$$

4.1 Large Darcy Number Case

For large Darcy numbers the velocity profile is given by Eq. (4-a) and the energy equation reads

$$\frac{d^2\theta}{dr^2}+\frac{1}{r}\frac{d\theta}{dr}+\frac{4Br}{3}\left(12r^2+s^2\left(6r^4-8r^2+3\right)\right)=0 \quad \text{with} \quad s^2<<1. \tag{10}$$

The solution to the above equation (by twice direct integration) subject to the boundary conditions (7-a) is

$$\theta = Br(1-r^4+s^2(2r^6-6r^4+9r^2-5)/9)+O(s^4). \tag{11}$$

The dimensionless bulk temperature may be found as

$$\theta_m = 5Br(1+2.3483s^2)/6+O(s^4). \tag{12}$$

To the first approximation, the dimensionless bulk temperature is θ_m=5*Br*/6 and the value *Br*=6/5 can be supposed as the threshold value beyond which viscous dissipation effect completely dominates over the wall heat transfer rate as a result of isothermal heating, for large Darcy number case.

Finally, the Nusselt number may be found as

$$Nu=48(1-2.515s^2)/5+O(s^4). \tag{13}$$

With large *Da*, i.e. when $s\to 0$, the velocity profile tends to be a parabolic one, which is known to be the plane Poiseuille flow solution, and $\theta\to Br(1-r^4)$. In the asymptotic region, $Nu\to 48/5$ similar to what reported in [23].

4.2 Small Darcy Number Case

For small Darcy numbers the velocity profile is given by Eq. (4-b) and the energy equation reads

$$\frac{d^2\theta}{dr^2}+\frac{1}{r}\frac{d\theta}{dr}+Br^*(1-2r^{-0.5}e^{-s(1-r)}+(4-7r^{-0.5}e^{-s(1-r)})/s)=0 \quad \text{with} \quad s>>1. \tag{14}$$

where *Br** is the Darcy-Brinkman number related to the clear fluid Brinkman number applied so far as $Br^*=Brs^2$. The solution to the above equation subject to the boundary conditions (7-a) is

$$\theta=\frac{Br^*}{4}(1+\frac{4}{s})(1-r^2)+O(s^{-2}). \tag{15}$$

This solution is obtained by twice direct integration by part [28] with the dimensionless bulk temperature

$$\theta_m=\frac{Br^*}{8}(1+\frac{6}{s})+O(s^{-2}). \tag{16}$$

For small Darcy numbers the dimensionless bulk temperature is approximately $\theta_m=Br^*/8$ and the value *Br**=8 can be supposed as the threshold value beyond which viscous dissipation effect completely dominates over the wall heat flux as a result of isothermal wall heating.

One finds the Nusselt number as

$$Nu=8(1-2/s). \tag{17}$$

As a check on our solution, we recover the known analytical solution for the limiting cases when *Da* is very small. Very small *Da* is equivalent to say for large values of *s* ($s\to\infty$), the velocity tends to a slug one, and $\theta\to 0.25\,Br^*(1-r^2)$ with $Nu\to 8$ which are in good agreement with those of Darcy model [20-22].

4.3 Entropy Generation

The entropy generation rate per unit volume can be found as

$$\dot{S}_{gen}=HTI+FFI\ , \tag{18}$$

where HTI and FFI may be found as

$$HTI = k\nabla T^*.\nabla T^*/T^{*2}, \quad FFI = \mu\phi/T^*. \tag{19-a,b}$$

The Bejan number, a measure of irreversibility due to heat transfer, is defined to be

Be=HTI/(HTI+FFI). (20)

Applying the dimensionless variables, the dimensionless entropy generation rate, *Ns*, and the Bejan number, *Be*, can be found as

$$Ns = \frac{\frac{1}{Pe^2}(\frac{\partial\theta}{\partial x})^2 + (\frac{\partial\theta}{\partial r})^2 + \frac{Br}{N}(1+N\theta)(s^2\hat{u}^2 + (\frac{d\hat{u}}{dr})^2)}{(\theta+1/N)^2}, \tag{21-a}$$

$$Be = ((\frac{\partial\theta}{\partial x})^2 + Pe^2(\frac{\partial\theta}{\partial r})^2)/((\frac{\partial\theta}{\partial x})^2 + Pe^2(\frac{\partial\theta}{\partial r})^2 + \frac{Br}{N}Pe^2(1+N\theta)(s^2\hat{u}^2 + (\frac{d\hat{u}}{dr})^2)). \tag{21-b}$$

where N is the dimensionless temperature difference $N=(T_{IN}-T_w)/T_w$.

Average values of *Ns* and *Be* are defined as $Ns^*=\langle Ns\rangle$ and $Be^*=\langle Be\rangle$ (the angle brackets show an average taken over the flow region).

Applying the asymptotic velocity and temperature profiles, one finds *Ns* and *Be* for very small *s* as

$$Ns = \frac{16(r^6 + r^2 + \frac{(1-r^4)BrN+1}{16BrN}) + \frac{s^2}{9}(-96r^8 + 194r^6 - 78r^4 + 87r^2 + 29)}{(\frac{1}{BrN} + 1 - r^4)((\frac{1}{BrN} + 1 - r^4) + \frac{s^2}{9}(4r^6 - 12r^4 + 18r^2 - 10))},$$
$$Be = \frac{r^6 - s^2(2r^8 - 4r^6 + 3r^4)/3}{(r^6 + r^2 + \frac{(1-r^4)BrN+1}{16BrN}) + \frac{s^2}{144}(-96r^8 + 194r^6 - 78r^4 + 87r^2 + 29)}. \tag{22-a,b}$$

On the other hand, for very large values of *s* one finds *Ns* and *Be* as

$$Ns = 4\frac{1 + \frac{4}{NBr^*} - \frac{16}{NBr^*s}}{(1 - r^2 + \frac{4(1-4/s)}{NBr^*})^2},$$
$$Be = \frac{r^2}{1 + \frac{4}{NBr^*} - \frac{16}{sNBr^*}}. \tag{23-a,b}$$

5. Results and Discussion

In this problem there are a large number of parameters to vary so that we restrict our results to the Nusselt number, the dimensionless entropy generation rate, and the Bejan number. Figure 1-b shows the developing Nusselt number for some values of the Darcy-Brinkman number and two values of *s*. One observes that while the asymptotic Nusselt number is independent of *Br** it depends on the value of *s*. It is also interesting that when one neglects the viscous dissipation effects the Nusselt number increases with an increase in s. On the other hand, for non-zero *Br** the Nusselt number decreases with an increase in *s*, similar to [29] which concerned flow through a parallel plate porous channel. Figure 1-c shows the asymptotic Nusselt number versus s for non-zero *Br** values. One observes that in the limit of very small or very large *s* values, our perturbation solution for *Nu* is in good agreement with the thermal entrance solution obtained numerically. Moreover, one notes that *Nu* stands between 8 and 48/5 for slug and clear flow case, respectively. Viscous dissipation changes the nature of the asymptotic flow and also the limits of the Nusselt number to the aforementioned values instead of 3.66 for plane Poiseuille flow and 5.78 for the Darcy model, as noted by Nield and Hooman [30] for similar problems.

Figures 2-3 show *Be* and *Ns*. We fixed the value of *N* to be small (*N*=0.01) so that the effects of property variation can be neglected. Besides, though *Pe* did not affect our temperature distribution, it will enter our calculation when it comes to investigate the Second Law aspects of the problem through the axial conduction term. We assumed *Pe*=10 knowing that moving form *Pe*=10 to *Pe*=100 will not alter *Nu* significantly [21], and [31-33]. However, more work is needed to examine relative importance of each term (for different flow and geometry conditions) in the thermal energy equation on top of recent numerical progress in the field of convection in porous media, see for example [34-42].

Figures 2-a/b show *Ns/Be* versus *r* at some axial locations with some *Br* values for *s*=10 while Figs. 3-a-c do the same for a smaller value of s corresponding to a hyperporous medium case, i.e. *s*=1. For a better understanding of the problem two separate figures are presented to show the *Be* plots, being Figs. 3-b,c. According to Fig. 2-a, *Ns* decreases from a high value at the wall (where both temperature and velocity gradients attain their maximum values) passes through a minimum, and then increases toward the tube center. It is worthy of noting that the minimum in *Ns* is associated with a maximum in *Be* as shown in Fig. 2-b. The streamwise variations of *Ns* become more pronounced as *Br* increases. However, for *Br*=10 the situation changes in such a way that *Ns* decreases form the wall to a minimum taking place at the tube centerline. This change in the trend of *Ns* is justified when one observes that when *Br*=10 the Bejan number is higher than those corresponding to smaller *Br* values. Moreover, for this case one verifies that *Be*>0.5 in the near wall region (*r*>0.7) that means HTI>FFI. However, for *r*<0.7 one realizes that HTI<FFI since the transverse temperature gradient will vanish while the Darcy dissipation rate reaches its maximum value at the tube center which is far away from the walls. Another feature of considerable interest is that when *Br*→0, not only $Be \neq 1$ but also the *Be* value becomes very small. This is justified when one observes that for the asymptotic region the temperature profile is a linear function of *Br*, i.e. with *Br*=0 both HTI and FFI would vanish and this can be verified using the corresponding plots of *Ns* in Fig. 2-a.

Based on Fig. 3-a, one observes that *Ns* plots show a monotonic increase from the tube center to the wall but the streamwise changes in *Ns* values are not very significant. A similar trend is observed in *Be* plots in Figs. 3-b,c. However, for *Br*=0.1 the situation changes in such a way that *Be* decreases down the channel unlike the other two cases with higher *Br* values. This means that for this value of *Br*, HTI<FFI down the channel.

Figures 4-a,b show an increase in *Ns** or *Be** with an increase in either *s* or *Br*. The only exception is the case *s*=1 where *Be** decreases slightly when *Br* increases from 0.1 to 1. This fact is in line with Fig. 3.

Acknowledgments

The first author, the scholarship holder, acknowledges the financial support provided by The University of Queensland in terms of UQILAS, Endeavor IPRS, and School Scholarship.

References

[1] K. Hooman, K., A.A. Ranjbar-Kani, A perturbation based analysis to investigate forced convection in a porous saturated tube, Journal of Computational and Applied Mathematics 162 (2) (2004) 411-419.

[2] D.A. Nield, A., Bejan, Convection in Porous Media, third ed., Springer-Verlag, New York, 2006.

[3] S. Mahmud, R. A. Fraser, Entropy-energy analysis of porous stack: steady state conjugate problem, International Journal of Exergy, 1 (3) (2004) 385-398.

[4] S. Mahmud, R. A. Fraser, The second law analysis in fundamental convective heat transfer problems, International Journal of Thermal Sciences, 42 (1) (2003) 177-186.

[5] K. Hooman, Analysis of entropy generation in porous media imbedded inside elliptical passages, International Journal of Heat and Technology, 23 (2) (2005) 141-145.

[6] K. Hooman, A. Ejlali, Second law analysis of laminar flow in a channel filled with saturated porous media: a numerical solution, Entropy, 7 (4) (2005) 300-307.

[7] K. Hooman, Second law analysis of thermally developing forced convection in a porous medium, Heat Transfer Research, 36 (6) (2005) 437-447.

[8] K. Hooman, Fully developed temperature distribution in a porous saturated duct of elliptical cross-section, with viscous dissipation effects and entropy generation analysis, Heat Transfer Research, 36 (3) (2005) 237-245

[9] A.C. Baytas, Entropy generation for free and forced convection in a porous cavity and a porous channel, in Eds. D.B. Ingham et al., Emerging Technology and Techniques in Porous Media , Kluwer Academic Publishers, 2004, pp. 259-270.

[10] B.A. Abu-Hijleh, Entropy generation due to cross-flow heat transfer from a cylinder covered with an orthotropic porous layer, Heat Mass Transfer, 39 (2) (2002) 27–40.

[11] A. Bejan, Entropy generation through heat and fluid flow, Wiley, New York, 1982.

[12] A. Bejan, Convection Heat Transfer, Wiley, New York, 1984.

[13] A. Bejan, Advanced Engineering Thermodynamics, second ed., Wiley, New York, 1997.

[14] A. K. Al-Hadhrami, L. Elliot, D.B. Ingham, A new model for viscous dissipation in porous media across a range of permeability values, Transport in Porous Media, 53 (1) (2003) 117-122.

[15] D.A. Nield, Resolution of a paradox involving viscous dissipation and nonlinear drag in a porous medium, Transport in Porous Media, 41 (3) (2000) 349-357.

[16] D.A. Nield, Modelling fluid flow in saturated porous media and at interfaces, in D. B. Ingham and I . Pop, eds., Transport Phenomena in Porous Media II, Elsevier Science, Oxford, 2002.

[17] D.A. Nield, Comments on ‘A new model for viscous dissipation in porous media across a range of permeability values’, Transport Porous Media, 55 (2) (2004) 253-254.

[18] K. Hooman, A. Pourshaghaghy, A. Ejlali, Viscous dissipation effects on thermally developing forced convection in a porous saturated circular tube, Applied Mathematics and Mechanics –English edition, 27 (5) (2006) 617-626

[19] K. Hooman, M. Gorji-Bandpy, Laminar dissipative flow in a porous channel bounded by isothermal parallel plates, Applied Mathematics and Mechanics –English edition, 26 (5) (2005) 587-593.

[20] K. Hooman, A.A. Ranjbar-Kani, A perturbation solution for laminar dissipative flow in a porous-saturated pipe with uniform wall temperature, with viscous dissipation effects, International Journal of Transport Phenomena, 6 (4) (2004) 307-313.

[21] A.V. Kuznetsov, M. Xiong, D.A. Nield, Thermally developing forced convection in a porous medium: circular duct with walls at constant temperature, with longitudinal conduction and viscous dissipation effects, Transport in Porous Media, 53 (3) (2003) 331-345.

[22] A. Haji-Sheikh, W. J. Minkowycz, E. M. Sparrow, A numerical study of the heat transfer to fluid flow through circular porous passages, Numerical Heat Transfer Part A, 46 (10) (2004) 929-955.

[23] R.K. Shah, A.L. London, Laminar Flow Forced Convection in Ducts (Advances in Heat Transfer, Supplement 1), Academic press, New York, 1978.

[24] E. Magyari, D.A.S. Rees, B. Keller, Effect of viscous dissipation on the flow in fluid saturated porous media, in K. Vafai, ed., Handbook of Porous Media, Taylor and Francis, New York, 2005, pp. 373-407.

[25] J.C., Tannehill, D.A. Anderson, R.H. Pletcher, Computational Fluid Mechanics and Heat Transfer, second ed., Taylor & Francis, 1997.

[26] A.A., Ranjbar-Kani, K. Hooman, Viscous dissipation effects on thermally developing forced convection in a porous medium: circular duct with isothermal wall, International Communications in Heat and Mass Transfer, 31 (6) (2004) 897-907.

[27] D.A. Nield, A.V. Kuznetsov, Forced convection in porous media: transverse heterogeneity effects and thermal development, in K. Vafai, ed., Handbook of Porous Media, Taylor and Francis, New York, 2005, pp. 143-193.

[28] A.H. Nayfeh, Problems in perturbation, second ed., Wiley, New York, 1993.

[29] K. Hooman, H. Gurgenci, Effects of viscous dissipation and boundary conditions on forced convection in a channel occupied by a saturated porous medium, Transport in Porous Media, in press.

[30] D.A., Nield, K. Hooman, Comments on “Effects of viscous dissipation on the heat transfer in forced pipe flow. Part 1: both hydrodynamically and thermally fully developed flow, and Part 2: thermally developing flow” by O. Aydin, Energy Conversion and Management, 47 (18-19) (2006) 3501-3503.

[31] K. Hooman, A.A. Ranjbar-Kani, A. Ejlali, Heat transfer to liquid metal flow in a porous saturated circular tube with uniform wall temperature: an exact solution, Heat Transfer Research, 34 (5-6) (2003) 304-309.

[32] K. Hooman, A.A. Ranjbar-Kani, A. Ejlali, Axial conduction effects on thermally developing forced convection in a porous medium: circular tube with uniform wall temperature, Heat Transfer Research, 34 (1-2) (2003) 34-40.

[33] K. Hooman, A.A. Merrikh, Analytical solution of forced convection in a duct of rectangular cross section saturated by a porous medium, ASME Journal of Heat Transfer, 128 (6) (2006) 596-600.

[34] A. Haji-Sheikh, D.A. Nield, K. Hooman, Heat transfer in the thermal entrance region for flow through rectangular porous passages, International Journal of Heat and Mass Transfer, 49 (17-18) (2006) 3004-3015.

[35] A.R.A. Khaled, K. Vafai, Analysis of flow and heat transfer inside nonisothermal squeezed thin films, Numerical Heat Transfer Part A, 47 (10) (2005) 981-996.

[36] S.V. Iyer, K. Vafai, Passive heat transfer augmentation in a cylindrical annulus utilizing a porous perturbation, Numerical Heat Transfer Part A, 36 (2) (1999) 115-128.

[37] M. KarimiFard, M.C. Charrier-Mojtabi, K. Vafai, Non-Darcian effects on double-diffusive convection within a porous medium, Numerical Heat Transfer Part A, 31 (8) (1997) 837-852.

[38] D.A.S. Rees, K. Vafai, Darcy-Brinkman free convection from a heated horizontal surface, Numerical Heat Transfer Part A, 35 (2) (1999) 191-204.

[39] D.A.S. Rees, M.A. Hossain, Combined effect of inertia and a spanwise pressure gradient on free convection from a vertical surface in porous media, Numerical Heat Transfer Part A, 36 (7) (1999) 725-736.

[40] S.S. Mousavi, K. Hooman, Heat and fluid flow in entrance region of a channel with staggered baffles, Energy Conversion and Management, 47 (15-16) (2006) 2011-2019

[41] P. Malekzadeh, H. Rahideh, G. Karami, A differential quadrature element method for nonlinear transient heat transfer analysis of extended surfaces, Numerical Heat Transfer Part A, 49 (5) (2006) 511-523.

[42] K. Khanafer, K. Vafai, Double-diffusive mixed convection in a lid-driven enclosure filled with a fluid-saturated porous medium, Numerical Heat Transfer Part A, 42 (5) (2002) 465-486.

Figure Captions:

Figure 1-a Definition sketch

Figure 1-b Developing Nu versus x for some values of s and Br*.

Figure 1-c The asymptotic Nusselt number versus s for non-zero Br* values

Figure 2-a/b Ns/Be versus r at some axial locations with some Br values (s=10)

Figure 3-a Ns versus r at some axial locations with some Br values (s=1)

Figure 3-b,c Be versus r at some axial locations with some Br values (s=1)

Figures 4-a/b Ns*/Be* versus Br for some values of s

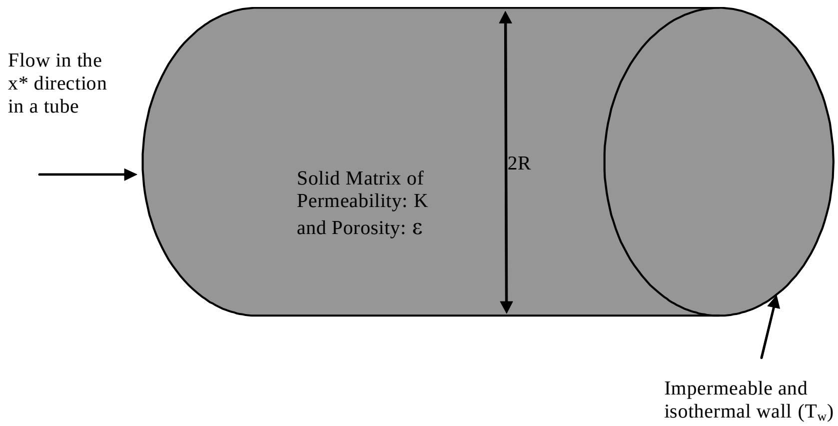

Fig. 1-a Definition sketch

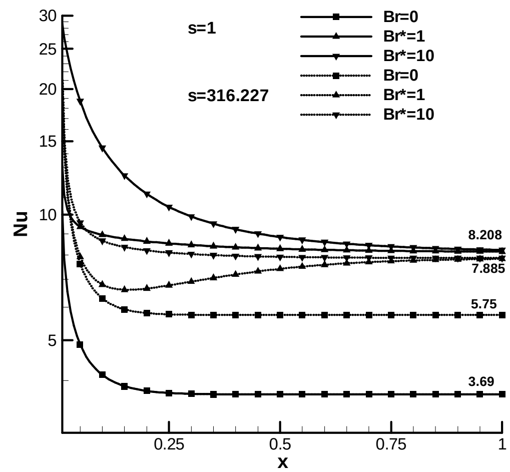

Fig. 1-b Developing Nu versus x for some values of s and Br*.

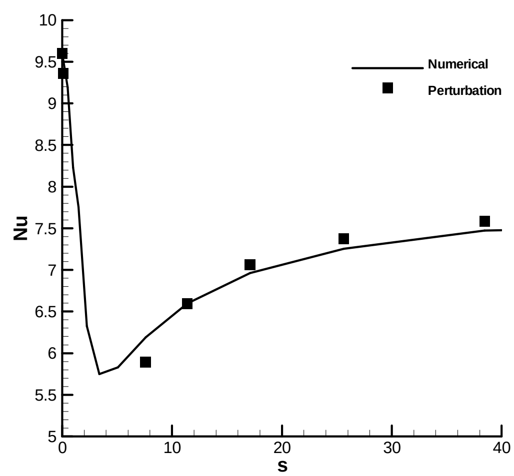

Fig. 1-c The asymptotic Nusselt number versus s for non-zero Br* values

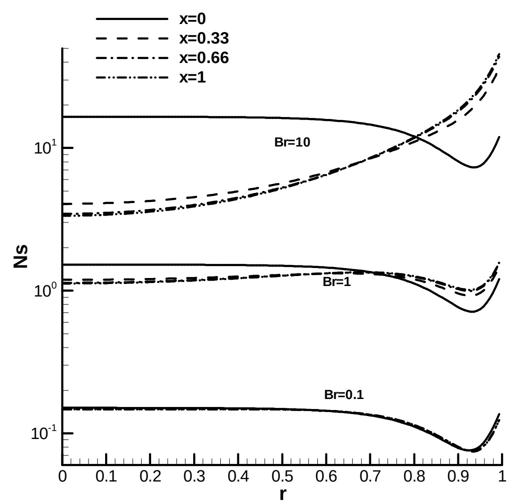

a)

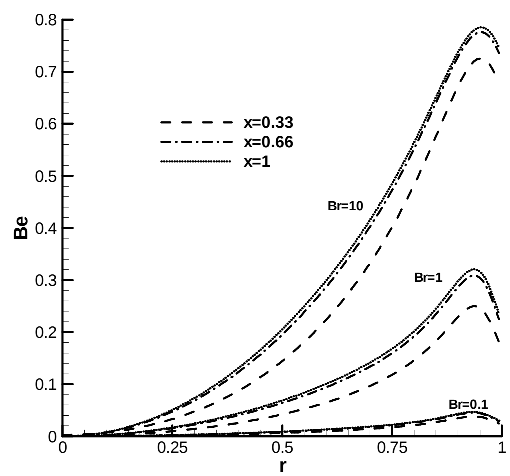

b)

Fig. 2-a/b Ns/Be versus r at some axial locations with some Br values (s=10)

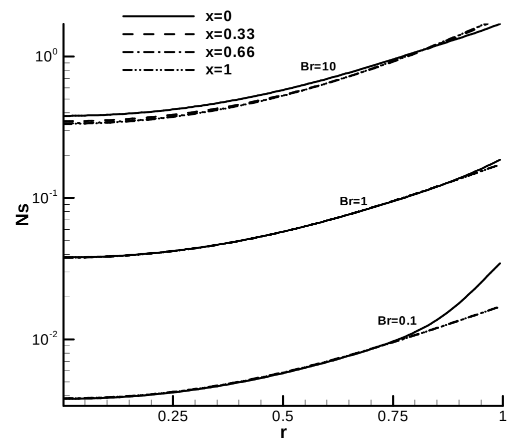

Fig. 3-a Ns versus r at some axial locations with some Br values (s=1)

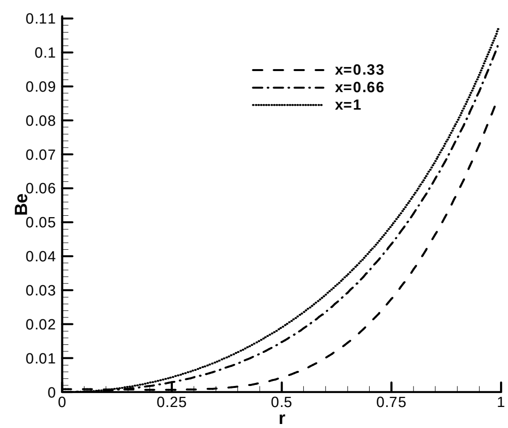

b) Br=10

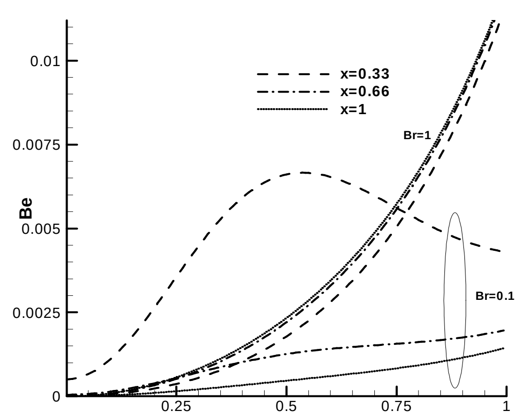

c) Br= 0.1 , 1

Fig. 3-b,c Be versus r at some axial locations with some Br values (s=1)

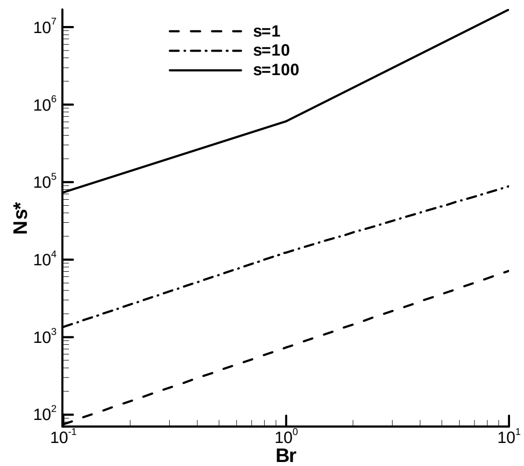

a)

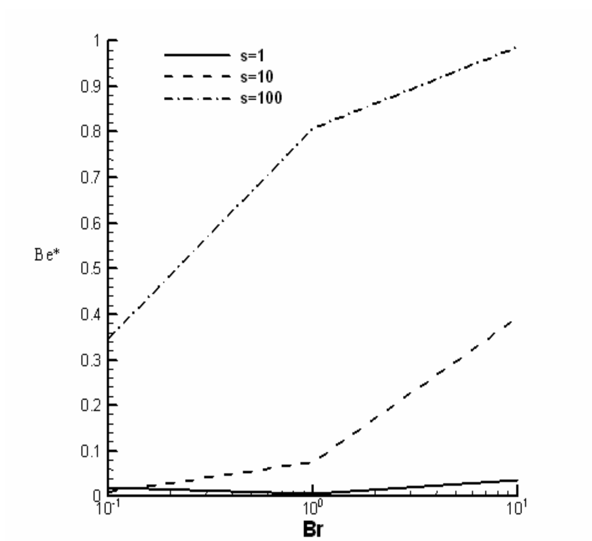

b)

Fig. 4-a/b Ns*/Be* versus Br for some values of s